Soil Dynamics and Earthquake Engineering 45 (2013) 96–111

Contents lists available at SciVerse ScienceDirect

Soil Dynamics and Earthquake Engineering

journal homepage: www.elsevier.com/locate/soildyn

Evaluation of the effect of earthquake frequency content on seismic behavior of cantilever retaining wall including soil–structure interaction

Tufan Cakir*

Department of Civil Engineering, Gümüşhane University, 29000 Gümüşhane, Turkey

ARTICLE INFO

Article history:
Received 20 April 2012
Received in revised form
21 November 2012
Accepted 22 November 2012
Available online 20 December 2012

ABSTRACT

A three-dimensional backfill–structure–soil/foundation interaction phenomenon is simulated using the finite element method in order to analyze the dynamic behavior of cantilever retaining wall subjected to different ground motions. Effects of both earthquake frequency content and soil–structure interaction are evaluated by using five different seismic motions and six different soil types. The study mainly consists of three parts. In the first part, following a brief review of the problem, the finite element model with viscous boundary is proposed under fixed-base condition. In the second part, analytical formulations are presented by using modal analysis technique to provide the finite element model verification, and reasonable agreement is found between numerical and analytical results. Finally, the method is extended to further investigate parametrically the effects of not only earthquake frequency content but also soil/foundation interaction, and nonlinear time history analyzes are carried out. By means of changing the soil properties, some comparisons are made on lateral displacements and stress responses under different ground motions. It is concluded that the dynamic response of the cantilever wall is highly sensitive to frequency characteristics of the earthquake record and soil–structure interaction.

1. Introduction

A main goal in seismic design of structures is to make sure that the structure has acceptable performance when it is subjected to ground motions with various intensities and probability of occurrences during its service lifespan. Study of seismic behavior is also essential for the safe design of cantilever walls in the seismic zone since they are widely used as soil retaining systems supporting fill slopes adjacent to roads and residential areas [1]. Many researchers have proposed several seismic analysis and design methods for retaining walls by using different approaches. Even though the quest for reasonable analysis and design methods of retaining structures has been pursued for many years, deformations ranging from slight displacement to catastrophic failure have been observed, and seismically induced retaining wall failures have been reported during the recent major earthquakes incorporating the 1999 Ji–Ji earthquake [2], the 2004 Chuetsu earthquake [3], and the 2008 Wenchuan earthquake [4].

The available methods that have been used for seismic analysis of retaining walls can conveniently be classified into three main categories [5]: (1) those are the traditional approaches developed for verifying geotechnical and structural behavior of walls, in which the relative motions of the wall and backfill material are sufficiently large to induce a limit or failure state in the soil, (2) those in which the wall is essentially rigid and the ground motion is of sufficiently low intensity so that the backfill is presumed to respond within the linearly elastic manner, (3) those in which the soil behaves as a nonlinear, hysteretic material.

The most well-known methods of the first category are the Mononobe–Okabe (M–O) method [6,7] and its various variants [8–10], which have found widespread acceptance in codes (e.g., ATC [11], EC-8 [12]). Representatives of the second category are the contributions of Matsuo and Ohara [13], Wood [14,15], Arias et al. [16], Veletsos and Younan [5,17–19], and Younan and Veletsos [20]. By definition, elastic solutions do not consider the true nonlinear hysteretic behavior of the soil, and they are not applicable to walls that can slide [21]. Therefore, in the third category, the finite element method is usually employed to analyze soil–wall systems [22]. Representatives of the third category are the contributions of Siddharthan et al. [23], Siller et al. [24], Elgamal and Alampalli [25], Al-Homoud and Whitman [26,27]. Moreover, the accuracy of the elastic solutions has been verified with finite element analyzes carried out by Wu and Finn [28] and Psarropoulos et al. [29]. Theodorakopoulos et al. [22,30] and Theodorakopoulos [31] examined the seismic response of a rigid wall retaining a semi-infinite and uniform soil modeled as a two-phase poroelastic medium. Lanzoni et al. [32] presented a simple method for seismic analysis of a flexible wall retaining a

* Tel.: +90 4562337425; fax: +90 4562337427.
E-mail address: cakirtufan@hotmail.com

0267-7261/$ - see front matter © 2012 Elsevier Ltd. All rights reserved.
http://dx.doi.org/10.1016/j.soildyn.2012.11.008

layer of fluid-saturated viscous and poroelastic soil. Elgamal et al. [33] investigated the dynamic characteristics of cantilever wall–backfill system through finite element analysis and forced vibration tests. Madabhushi and Zeng [34] presented the results of both finite element simulation and centrifuge test of a flexible cantilever wall. Mylonakis et al. [35] and Evangelista et al. [36] proposed stress plasticity solutions for evaluating earth pressure coefficients. Stamos and Beskos [37] studied the dynamic response of infinitely long lined tunnels by a special direct boundary element method. Hatzigeorgiou and Beskos [38] investigated the seismic response of 3-D tunnels by assuming inelastic material behavior and considering soil–structure interaction. Cakir and Livaoglu [39] presented a simplified seismic analysis procedure for analysis of backfill-rectangular tank-fluid systems.

Considering previous studies, it is seen that most of them have focused on the determination of earthquake-induced earth pressures. However, limited research has been done on the effects of soil–structure interaction and earthquake frequency content on seismic behavior of cantilever walls in three dimensional space. Due to the importance of these critical parameters, a new study is necessary to investigate the effects of them on the response. As for the codes (e.g., TEC [40], IS 1893 [41], EC-8 [42]) about retaining structures, it is obvious that the analyzes of them are generally carried out by using pseudo-static approximations although these approaches do not properly consider the interaction effects.

The aim of this paper is three-fold: (a) after a brief review of the problem, to present details of finite element model of the system under investigation, (b) to verify the validity of it under fixed-base and elastic soil assumptions through the proposed analytical model, (c) to further investigate the seismic behavior of cantilever wall considering the effects of soil–structure interaction and earthquake frequency content.

Five different ground motions including 1979 Imperial Valley, 1983 Coalinga, 1987 Whittier Narrows, 1989 Loma Prieta and 1994 Northridge are applied to consider the effect of frequency content. All records are scaled in such a way that the horizontal peak ground acceleration reaches 0.37 g. The frequency content characteristic of the ground motion is reflected in predominant period, bandwidth, central frequency, power spectrum intensity, the ratio of peak ground velocity to peak ground acceleration (PGV/PGA), response spectrum intensity, velocity spectrum intensity and acceleration spectrum intensity etc. [43]. Accordingly, consideration of the frequency content can be raised through different ways. Although PGA and PGV are very useful intensity measures for seismological studies, none can provide any information on the frequency content. PGA and PGV have to be supplemented by additional information for the proper characterization of a ground motion [44]. In this connection, the ratio of PGV to PGA is a ground motion parameter which provides information about frequency content. Because PGA and PGV are usually associated with motions of different frequency, the ratio should be related to the frequency content of the motion [45,46]. Furthermore, Tso et al. [47] have shown that the ratio of PGA/PGV indicates the relative frequency content of the ground motion. So, a good indicator of the frequency content is the ratio of PGA which is expressed in units g to PGV expressed in units m/s. Earthquake records may be classified into three groups according to the frequency content ratio: (a) high PGA/PGV ratio when $PGA/PGV > 1.2$, (b) intermediate PGA/PGV ratio when $1.2 \geq PGA/PGV \geq 0.8$, (c) low PGA/PGV ratio when $PGA/PGV < 0.8$. [48]. The Loma Prieta record has low frequency content, the Imperial Valley and Northridge earthquakes have intermediate frequency contents, and the Coalinga and Whittier Narrows records have high frequency contents. It can be expressed here that because of the complexity of the response of soil–wall–backfill system, normalization by using the fundamental periods of the wall may lead to misleading results. The considered system response includes the contribution of different parts like backfill and soil foundation responses. Scaling the records in such a way, or in other words, normalization by taking only wall response into account may cause to ignore other effects. Therefore, the abovementioned normalization technique has been selected in this study. However, it should be stated that the best way for normalization is to use the fundamental periods of the system, if the first mode almost controls and characterizes all system response.

2. Problem definition

The problem under investigation consists of a uniform layer of elastic material, that is free at its upper surface, bonded to a non-deformable rigid base and retained along one of its vertical boundaries by a uniform cantilever wall that is considered to be fixed at the base and to be free at the top. The heights of the wall and soil stratum are considered to be the same, and they are denoted by H. The properties of the soil stratum are defined by its mass density, shear modulus of elasticity, Poisson's ratio. The properties of the structural wall are defined by its thickness, mass density, moment of inertia, Young's modulus and Poisson's ratio. Furthermore, dry-cohesionless soil is considered in the analyzes. The scheme of the backfill–cantilever wall system examined is shown in Fig. 1.

3. Finite element modeling

The main advantage of the FEM in analyzing a soil–structure interaction problem is that it can accommodate easily for heterogeneity in the soil or structure medium and for nonlinearity in the materials, as well as in the geometry. Most of the finite element numerical codes perform analyzes in time domain, allowing the introduction of specialized constitutive laws describing the linear and nonlinear behavior of the soil under strong ground motions [49]. In this connection, the proposed numerical model for the problem under fixed-base assumption is depicted in Fig. 2. It should be noted here that the finite element modeling and analyzes were carried out by using the commercial software, ANSYS [50]. The literature review shows that to simplify the soil–structure interaction analysis, three-dimensional problems are often modeled by considering a two-dimensional slice with the same material properties. This assumption, although convenient, is potentially dangerous for the following reasons. First, the specific radiation damping per unit contact area calculated for the two-dimensional case overestimates the actual three-dimensional case for finite frequencies. Second, the contact area of a reasonably selected two-dimensional model will be larger than that of the three-dimensional case which will further increase radiation damping [51,52]. Accordingly, it is not possible to obtain a two-dimensional representation that will approximate

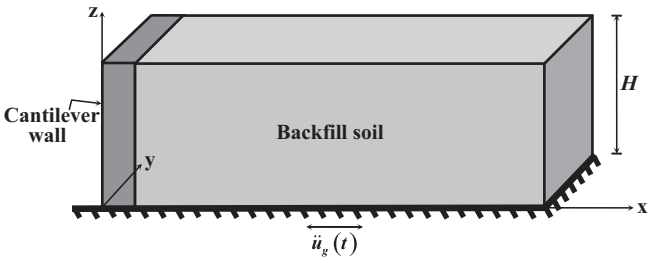

Fig. 1. System considered.

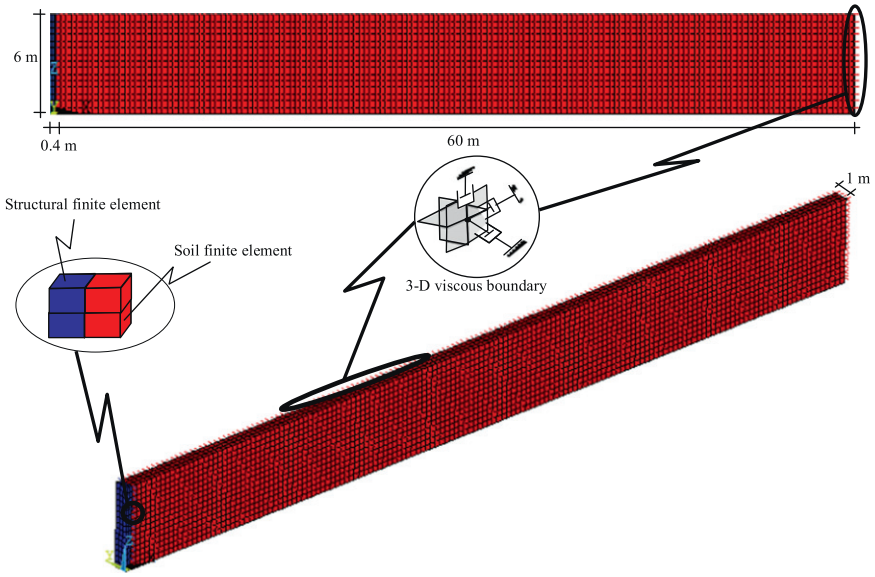

Fig. 2. Finite element modeling of backfill–cantilever wall system under fixed-base case.

both the dynamic stiffness and damping over a reasonable range of frequencies [53], and since the damping is grossly overestimated, two-dimensional modeling of a three-dimensional case cannot be recommended for actual engineering applications [51]. Therefore, the author has concentrated on the three-dimensional modeling of the interaction system for a cantilever wall length of 1 m in this study (see Fig. 2).

In the finite element modeling, the structural wall is modeled with solid elements defined by eight nodes having three translational degrees of freedom in each node. The soil stratum is also modeled with solid elements with eight nodes having three degrees-of-freedom at each node: translations in the nodal x, y, z directions. Regarding the backfill–wall interface, although the option of de-bonding was available in ANSYS, the assumption of complete bonding – made by both in the study of Veletsos and Younan and in the analytical model proposed by the author in this study – was also adopted to permit a comparative study at this stage. However, after providing the model validation by means of the proposed analytical model, comprehensive earthquake analyzes will be fulfilled considering not only effects of earthquake frequency content and soil interaction but also the behavior of backfill–wall interface in Sections 6 and 7.

In many earthquake engineering and seismological problems, wave propagation examinations in a large soil medium are necessary, and also the simulation of the infinite medium is an extremely important topic in the dynamic soil–structure interaction problems. The general approach of treating these problems is to divide the infinite medium into the near field (truncated layer), which includes the irregularity as well as the non-homogeneity of the soil adjacent to the structure, and the far field, which is simplified as an isotropic homogeneous elastic medium [54]. The finite element methods, being powerful in most engineering applications of normal size, are somewhat restrictive in the geotechnical area due to the large physical dimensions. Moreover, a full nonlinear three-dimensional finite element analysis is still very costly in terms of the computational efforts. As an alternative to modeling very large soil volumes and to limit the model to a reasonable size, special artificial and/or transmitting boundaries must be introduced in the finite element analysis of dynamic soil–structure interaction problems. This not only avoids unrealistic wave reflections against the artificial boundaries introduced in the mathematical model but also provides the consideration of

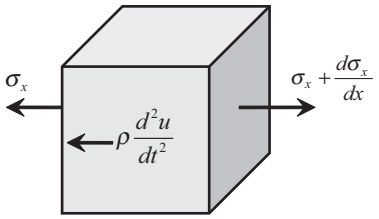

Fig. 3. Forces acting on unit cube [67].

radiation effects, and thus, the results are not distorted. Several artificial boundaries have been proposed in frequency and time domains in the case of solids. Lysmer and Kuhlemeyer [55] and Kuhlemeyer and Lysmer [56] suggest applying viscous tractions that must absorb reflected energy along the artificial boundary. The advantage of this approach lies in the fact that the applied stresses are frequency independent. This technique is widely used because it is easy to implement and gives satisfactory results for dilatational and shear waves. Later, different boundary models have been used and developed [57–64].

In this study, the viscous boundary model, which was successfully employed in the finite element modeling of the elevated and rectangular tanks performed by Livaoglu and Dogangun [65] and Livaoglu et al. [66], is used in three dimensions to consider radiational effect of the seismic waves through the soil medium. A plane wave propagating in the x-direction is considered to compute the properties of this boundary condition. The forces that cause wave propagation are shown acting on a unit cube depicted in Fig. 3.

The one dimensional equilibrium equation in the x-direction is:

$$\rho \frac{d^2u}{dt^2} - \frac{d\sigma_x}{dx} = 0 \tag{1}$$

Because $\sigma_x = E_c \varepsilon_x = E_c(du/dx)$, the one dimensional partial differential equation is written in the following classical wave propagation form:

$$\frac{d^2u}{dt^2} - v_p^2 \frac{d^2u_x}{dx^2} = 0 \tag{2}$$

where v_p is the wave propagation velocity of the material and is given by $v_p = \sqrt{E_c/\rho}$, in which ρ is the mass density and E_c is the bulk modulus. The solution of Eq. (2) for harmonic wave propagation in the positive x-direction is a displacement $u(t,x)$ of the following form:

$$u(t,x) = U\left[\sin\left(\omega t - \frac{\omega x}{v_p}\right) + \cos\left(\omega t - \frac{\omega x}{v_p}\right)\right] \tag{3}$$

The velocity of a particle $\dot{u}(t,x)$ at location x:

$$\dot{u}(t,x) = U\omega\left[\cos\left(\omega t - \frac{\omega x}{v_p}\right) - \sin\left(\omega t - \frac{\omega x}{v_p}\right)\right] \tag{4}$$

The strain in the x-direction is:

$$\varepsilon(x,t) = \frac{du}{dx} = -\frac{\dot{u}(x,t)}{v_p} \tag{5}$$

The corresponding stress can now be expressed in the following simplified form [67]. The same results were obtained by Lysmer and Kuhlemeyer [55].

$$\sigma(x,t) = E_c\varepsilon(x,t) = -\rho v_p \dot{u}(x,t) \tag{6}$$

The compression stress is identical to the force in a simple viscous damper with constant damping value equal to ρv_p per unit area of the boundary. Also, it can be easily shown that shear wave radiation boundary condition is satisfied if damping values are assigned to be ρv_s per unit of boundary area [67]. v_p and v_s are dilatational and shear wave velocity of the considered medium.

The viscous boundaries can be used with finite element mesh as depicted in Fig. 4 for three dimensional model. In this figure, A_n, A_{t1} and A_{t2} are the fields controlling the viscous dampers, σ and τ are the normal and shear stresses occurring in the boundaries of the medium, and the subscripts n and t represent normal and tangent directions in the boundary. When the viscous boundaries are taken into account, the well-known equation of motion can be written as follows:

$$[\mathrm{M}]\{\ddot{u}(t)\} + [\mathrm{C}]\{\dot{u}(t)\} + [\mathrm{C}^*]\{\dot{u}(t)\} + [\mathrm{K}]\{u(t)\} = \{P(t)\} \tag{7}$$

where $\mathbf{C}^*$ is the special damping matrix that may be considered as follows:

$$[\mathrm{C}^*] = \begin{bmatrix} A_n\rho v_p & 0 & 0 \\ 0 & A_{t1}\rho v_s & 0 \\ 0 & 0 & A_{t2}\rho v_s \end{bmatrix} \tag{8}$$

To represent the behavior of the semi-infinite backfill medium, the critical minimum distance from the face of the wall is taken as $10H$, a value which is believed to approximate adequately the behavior of the semi-infinite layer [5,29]. In this context, the dashpots were also placed $10H$ away from the wall in three dimensions to improve the accuracy of the simulation (see Fig. 2), where H is the height of the cantilever wall.

4. Analytical modeling

The condensation of the multi degree of freedom system to a system with fewer degrees of freedom is a common application in structural dynamics. This technique provides some appealing advantages such as the physical insight, conceptual clarity, the relative easiness of construction and the low computational effort, and may lead to sufficient engineering accuracy. Accordingly, the simple physical models can be used with a small number of degrees of freedom. In addition, these models can be constructed to check the results of rigorous methods such as the boundary element procedure or finite element method [68]. The three types of simple physical models – the spring–dashpot–mass models, the truncated cones and the method with a prescribed wave pattern in the horizontal plane – are examined in great detail in the study by Wolf [52].

In this study, a spring–dashpot–mass model with frequency-independent coefficients is introduced in order to demonstrate the obtainable accuracy of the finite element model. The simplified analytical model of cantilever wall retaining a soil stratum on rigid base is given in Fig. 5. The method presented by Veletsos and Younan [5] was adopted for the determination of the stiffness and mass values for backfill soil. Furthermore, the mass of the cantilever wall is taken into account, and the system is represented by spring–dashpot–mass model with two degrees of freedom in this study while Veletsos and Younan had regarded the wall as massless. The spring–dashpot–mass system is attached to the wall at a height $=0.637H$ where H is the height of the wall. To obtain a simplified model and to permit a comparative study, the approach is based on the simplifying assumption that complete bonding is presumed at the wall–soil interface. The considered problem can simply be idealized as in Fig. 5.

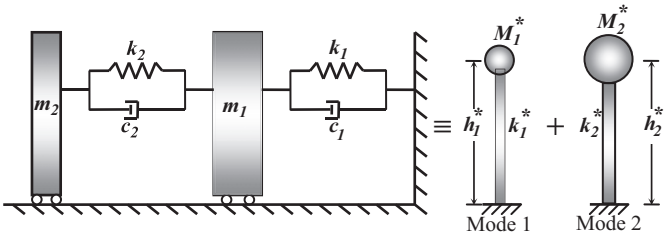

Fig. 5. Proposed spring–dashpot–mass model and modal representation of the system.

$$N_n = A_n\sigma_n\ ;\quad N_{t1} = A_{t1}\tau_{t1}\ ;\quad N_{t2} = A_{t2}\tau_{t2}$$
$$N_n + C_n\dot{u}_n = 0$$
$$N_{t1} + C_{t1}\dot{u}_{t1} = 0$$
$$N_{t2} + C_{t2}\dot{u}_{t2} = 0$$

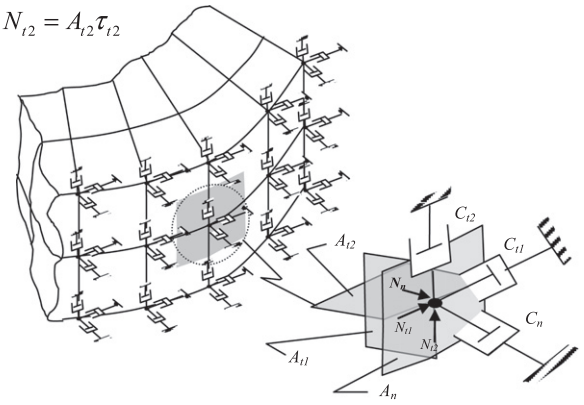

Fig. 4. Viscous boundaries in the 3-D finite element model [65].

The coefficients of the springs, dashpots and masses can be determined for varying parameters such as the dimensions, physical and mechanical properties of both soil and wall. To define the modal characteristics of the system, the corresponding design parameters as stiffnesses and masses of the system, must be introduced primarily. The mass m_1 refers to soil mass and is equal to

$$m_1 = 0.543\psi_\sigma \rho H^2 \tag{9}$$

where

$$\psi_\sigma = \frac{{\psi_0}^2}{\psi_e}; \quad \psi_0 = \sqrt{\frac{2}{1-\nu}}; \quad \psi_e = \sqrt{\frac{2-\nu}{1-\nu}} \tag{10}$$

where ρ is the mass density of soil, H is the height of both the wall and the soil stratum, ν is the Poisson's ratio for soil and ψ_σ, ψ_0, ψ_e are the functions of ν.

The spring stiffness k_1 for the model with constant parameters is

$$k_1 = m_1 \frac{\pi^2}{4H^2}\frac{G}{\rho} = 1.339\psi_\sigma G \tag{11}$$

where G is the shear modulus of elasticity of soil material.

The mass of the wall is represented by m_2, and the lateral stiffness of the wall, k_2, can easily be determined as $k_2 = 3EI/H^3$. The parameters of c_1 and c_2 are the damping values for backfill and structure, respectively.

The development of the simplified analytical solution may be derived from a physical interpretation of the solution to the differential equation. Considering dynamic equilibrium of the masses by using D'Alembert's principle, from Fig. 5, basic dynamic equations can be written in matrix form:

$$\begin{bmatrix} m_1 & 0 \\ 0 & m_2 \end{bmatrix}\begin{Bmatrix} \ddot{u}_1 \\ \ddot{u}_2 \end{Bmatrix} + \begin{bmatrix} c_1+c_2 & -c_2 \\ -c_2 & c_2 \end{bmatrix}\begin{Bmatrix} \dot{u}_1 \\ \dot{u}_2 \end{Bmatrix} + \begin{bmatrix} k_1+k_2 & -k_2 \\ -k_2 & k_2 \end{bmatrix}\begin{Bmatrix} u_1 \\ u_2 \end{Bmatrix} = \begin{Bmatrix} P_1(t) \\ P_2(t) \end{Bmatrix} \tag{12}$$

where (u_1, u_2), $(\dot{u}_1, \dot{u}_2)$, $(\ddot{u}_1, \ddot{u}_2)$ are the displacements, velocities and accelerations of masses m_1, m_2, respectively, and $P_1(t)$ and $P_2(t)$ are the external forces. It is worth stating that since the natural frequencies of the system in the modal analysis are determined by using undamped free vibration equation of motions, any data on both the damping matrix and the external forces are not given herein. However, these data will be included in Section 6, where the seismic analysis of the interaction system is performed by means of the finite element model.

The obtained equations can be solved by employing the modal analysis technique. For this, first, the modal properties such as effective modal masses (M_1^*, M_2^*), heights (h_1^*, h_2^*) and stiffnesses (k_1^*,k_2^*) must be determined (see Fig. 5). These modal properties can be estimated by using Eqs. (13) and (14) [69].

$$M_n^* = \Gamma_n L_n^h = \frac{\left(L_n^h\right)^2}{M_n}; \quad h_n^* = \frac{L_n^\theta}{L_n^h}; \quad k_n^* = \omega_n^2 M_n^* \tag{13}$$

where

$$M_n = \phi_n^T m \phi_n = \sum_{j=1}^{N} m_j \phi_{jn}^2; \quad \Gamma_n = \frac{L_n^h}{M_n}; \quad L_n^h = \sum_{j=1}^{N} m_j \phi_{jn};$$
$$L_n^\theta = \sum_{j=1}^{N} h_j m_j \phi_{jn} \tag{14}$$

where N, ϕ_n, and ω_n^2 are the total mode number, the $\boldsymbol{n}$th mode vector and its eigenvalue, respectively.

5. Numerical application and model verification

In this section, to verify the validity and applicability of the present finite element model, the modal analyzes of a cantilever wall–backfill system are performed. In the numerical example, a 6 m-high cantilever retaining wall with a constant thickness of 0.4 m is considered. As stated before, the critical minimum distance from the face of the wall is taken as $10H = 60$ m. The Young's modulus, Poisson's ratio and unit weight of the concrete were considered as 28,000 MPa, 0.2 and 25 kN/m^3, respectively. The Young's Modulus, Poisson's ratio and the unit weight of the soil were taken to be 50 MPa, 0.3 and 18 kN/m^3, respectively. The comparison between the numerically derived result and the analytical data is carried out, and a close match is also seen in this section.

A computer code was written by the author in order to obtain modal characteristics of the system via analytical model. The values of mass and stiffness, which are necessary to estimate the natural frequencies of the interaction system, are presented in Fig. 6. The modal characteristics such as the effective modal masses, stiffnesses and modal frequencies can also be seen in Fig. 6.

As Fig. 6 depicts, the mode frequencies were computed as 2.85 and 4.47 Hz. It should be noted here that the first and second modes represent the backfill and wall modes, respectively. 25% of the total effective mass is represented by the backfill mode, and 75% of it is represented by the structural mode. It means that the modes are adequate to represent all system behavior.

In addition, the modal characteristics of the same system can be determined by means of the proposed finite element model. Fig. 7 illustrates the mode shapes of the system. The first three vibration modes, which have the ability to represent all system behavior based on effective modal masses, were identified in this figure. The frequencies of the modes were estimated as 4.45, 4.89 and 5.61 Hz.

The frequency results obtained by the FEM simulation and the analytical model are seen in Table 1. It is worth saying here that only the comparison of the modes related to structure is given because this work is mainly focused on the cantilever wall behavior subjected to soil effects in accordance with the purpose of the study. In this connection, when a comparison is made for the first structural mode, it is seen that the trend of the present numerical result agrees well with analytical value so that the

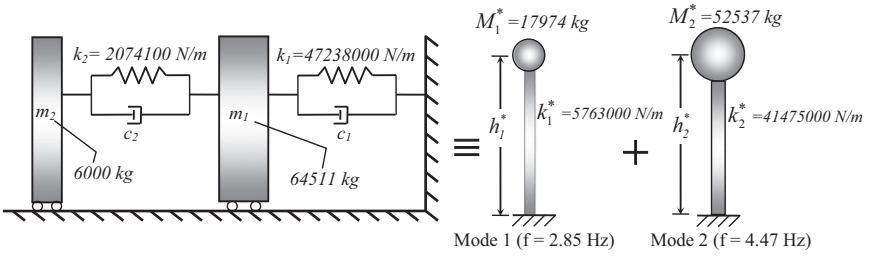

Fig. 6. Modal characteristics of backfill–cantilever retaining wall system.

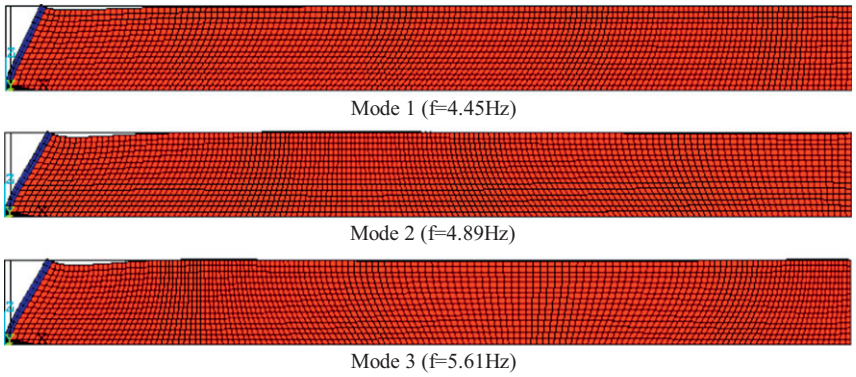

Fig. 7. Mode shapes and frequencies of the system obtained from finite element model.

Table 1
Analytical and numerical results.

Mode categories	Mode descriptions	Modal frequencies (Hz)	
		Analytical model	Finite element model
Backfill	Backfill mode	2.85	–
Structure	First mode	4.47	4.45
	Second mode	–	4.89
	Third mode	–	5.61

mode frequency is computed as 4.47 Hz from the analytical model while the same quantity is calculated as 4.45 Hz from the finite element model. In fact, this reveals successful estimation, the analytical verification provides strong support for the finite element model, and this makes the model attractive for use in further investigations.

6. Seismic analysis

After verifying the validity of the finite element simulation through the analytical model, the versatility of the finite element model allows the treatment of some more realistic situations that are not amenable to analytical solution. Therefore, the modeling was extended to account for the behavior of wall–soil interface, elasto-plastic behavior of soil and soil/foundation interaction effects.

Reasonable modeling of the wall–backfill interaction requires using special interface elements between the wall and adjacent soil. Thus, as a special interface element, nonlinear spring is used between the backfill and wall allowing for the opening and closing of the gaps (i.e., de-bonding and bonding) to model backfill–wall interaction. This is a unidirectional element with nonlinear generalized force-deflection capability that can be used in any analysis. The element has longitudinal or torsional capability in 1-D, 2-D, or 3-D applications. The longitudinal option is a uniaxial tension–compression element with up to three degrees of freedom at each node: translations in the nodal x, y, and z directions. The 1-D longitudinal option in the direction of normal to the wall is taken into account to simulate the behavior of backfill–cantilever wall interaction surface. In addition to the modeling of the superstructure, the soil/foundation system is also modeled with 3-D structural solid elements defined by eight nodes with three translational degrees-of-freedom in each node, and the artificial viscous boundaries have been placed in three dimensions on the boundaries of soil/foundation medium. Accordingly, the problem presented in Fig. 8 reveals a complex phenomenon that incorporates both the backfill and soil/foundation interaction effects. The proposed finite element model of the

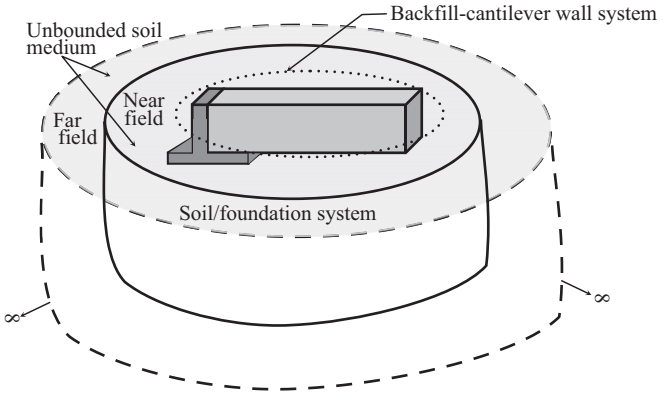

Fig. 8. The problem investigated for dynamic backfill–structure–soil/foundation interaction.

backfill–cantilever wall–soil/foundation interaction system is also shown in Fig. 9. Considering most of the methods proposed by the previous researchers, it is seen that the analyzes of retaining walls are generally carried out by using pseudo-static and/or pseudo-dynamic approximations. However, representation of the complex, transient, dynamic effects of earthquake shaking by a single constant unidirectional pseudo-static acceleration is quite crude. In the pseudo-dynamic approaches, the dynamic nature of the earthquake loading is also considered in an approximate and simple manner. Moreover, the pseudo-dynamic method uses an elastic wave solution in soil which is in a state of plastic deformation, and does not take into account the wave reflection at the soil free surface, and these may lead to an incomplete analysis for design purpose of the structure. On the other hand, despite these limitations it is evident that the conventional pseudo-static approach, which is very widely accepted and famous for its simple applicability to a wide range of problems, has continuously been used by the geotechnical engineers for design of retaining walls. As for the numerical modeling studies on retaining walls, it is clearly seen that most of them were done based on the two-dimensional analysis [27,29,36,59,70,71]. It may be possible to obtain close approximations to the system frequencies, by properly selecting the two-dimensional model. However, two-dimensional finite elements should not be used to solve three-dimensional soil–structure interaction problems, and two-dimensional representations may lead to underestimation of the peak response, as discussed at the end of the first paragraph in Section 3. Therefore, extension of 2-D analysis to 3-D analysis makes the problem more realistic. Furthermore, no de-bonding or relative slip is allowed to occur at the wall–soil interface in some of the studies. However, not modeling the de-bonding/recontact behavior at the interface between the wall and adjacent soil may

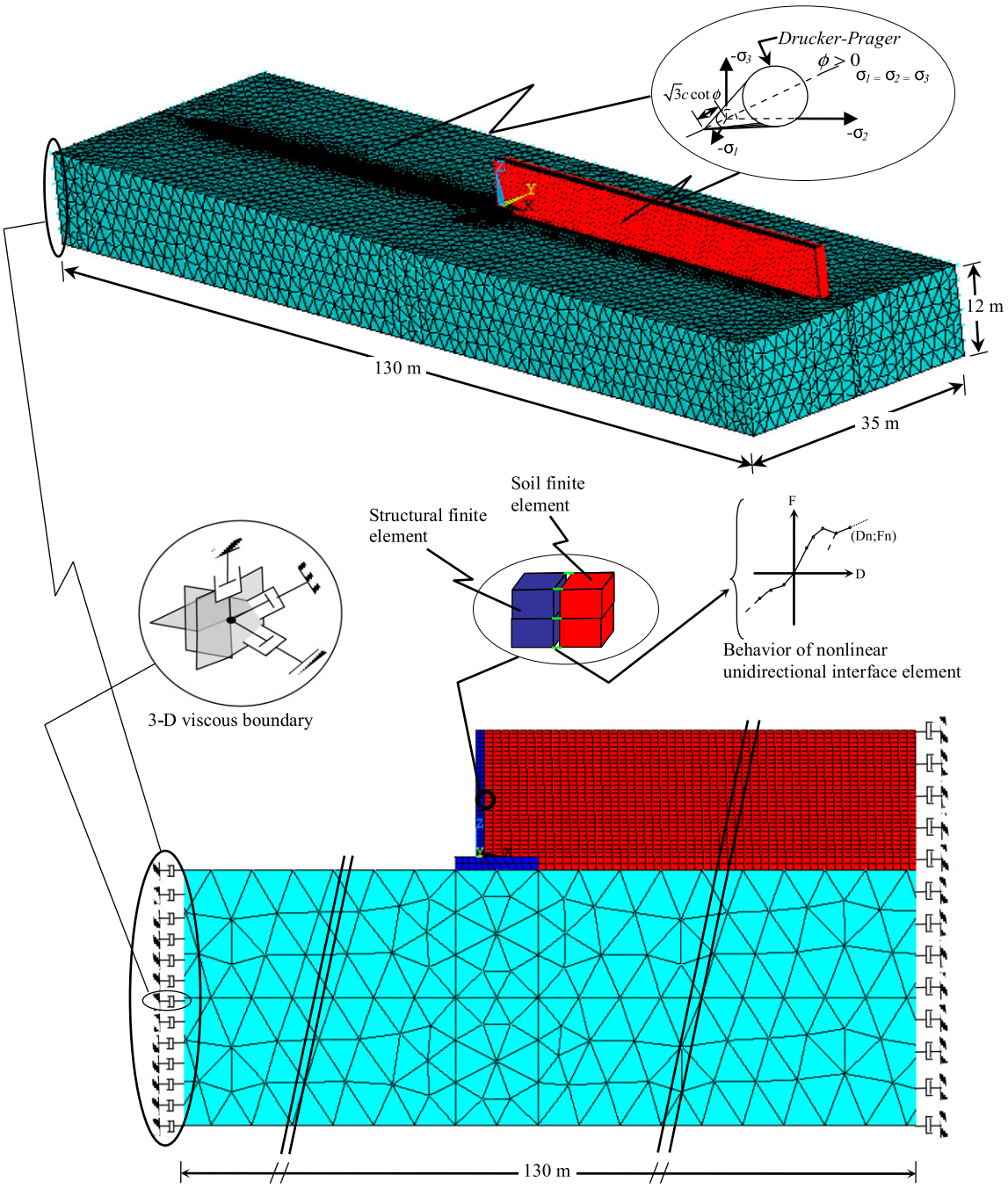

Fig. 9. Proposed finite element model for backfill–cantilever wall–soil/foundation interaction system.

be unrealistic. On the other hand, the problems associated with seismic behavior of cantilever retaining walls cover many fundamental parameters, and the issue of seismic behavior remains little explored. In fact, the seismic behavior of retaining walls is governed by earthquake motion characteristics, boundary conditions of the problem, backfill and foundation properties, structural wall properties, the interaction between backfill and structure as well as subsoil and structure along their boundaries [72,73]. The proposed 3-D finite element model can consider these aspects of the dynamic problem. It should be noted that the objective here is not to claim a strict validation of the model as many factors that play important role in the field cannot be truly accounted for. On the other hand, despite the complexities associated with accounting for interaction effects, the following analyzes show that the model can provide a reliable tool for performing parametric studies. In addition, more recently, some researchers have performed experimental measurements to investigate the dynamic behavior of cantilever retaining walls. In one of these studies, Kloukinas et al. [74] carried out a series of shaking table tests on scaled models of cantilever retaining walls to explore the dynamic behavior. First of all, it should be noted that, in the current subject, this investigation has great challenging and important results. The researchers showed that systematic amplification is occurred for all harmonic excitations following the stratigraphy, whereas the earthquake loading results to conditions closer to the assumptions of the pseudo-static analysis. There are some interesting points in conformity with the main idea of this paper. They observed that only the wall

responds during yielding under harmonic loading, whereas soil responds in a quite different way. Furthermore, the most important outcome of the study in earthquake loading highlights that a mass of soil moving together with the wall is evident. These evidences reveal the necessity of modeling the investigated system by taking both foundation-soil and backfill system together with the wall into consideration, and the necessity of investigations on effect of frequency content to the system. These differences between the earthquake loading and the harmonic one stem from the frequency content of earthquake loading. Therefore, as mentioned before, the main objective was selected to define the frequency content effect of ground motion on soil–foundation–wall–backfill model. In this context, the experimental study indicated once again that this is a proven need for soft soil conditions, especially for earthquake loading. Moreover, backfill interaction effect appeared as a much more decisive parameter for such a system as well as soil/foundation interaction.

It is well known that soil materials have a very complicated behavior. Idealizations are, therefore, often necessary in order to develop simple mathematical constitutive laws for practical applications. Although viscoelastic, elastoplastic and hypoplastic material models have been widely used in representing the behavior of different soil materials, material tests and existing database show that granular materials have scattered physical and mechanical properties which vary due to conditions. Even bulk mass density may change as 40% via moisture contents. On the other hand, the designers for special design and scientists for scientific purposes to the specific problem can use rigorous models, i.e., modified cam-clay model for clay and hypoplastic constitutive model for granular material. However, in this study, the main purpose was to investigate the seismic behavior of cantilever wall considering the effects of soil–structure interaction and earthquake frequency content. For such a purpose, the author did not consider to focus on the effects of specific properties of granular material like moisture content, void ratio, etc. In point of fact, one can easily find huge differences between the results by changing these properties within their range limits. To that end, by taking the aim into account, Drucker–Prager material model was used (see Fig. 9). Of course other smooth surfaces have been proposed but because of its simplicity and available computer codes for it, the Drucker–Prager model has gained popularity and are still used even for analyzing challenging projects in spite of some limitations of it.

In the nonlinear time history analyzes, 1979 Imperial Valley, 1983 Coalinga, 1987 Whittier Narrows, 1989 Loma Prieta and 1994 Northridge earthquakes are used as excitations in order to evaluate the effect of earthquake frequency content. The records are scaled in such a way that the horizontal peak ground acceleration reaches 0.37 g, as shown in Fig. 10. Furthermore, the properties of the ground motions are given in Table 2 [75]. As mentioned before, based on the ratio of peak ground acceleration (PGA) to peak ground velocity (PGV), the Loma Prieta record

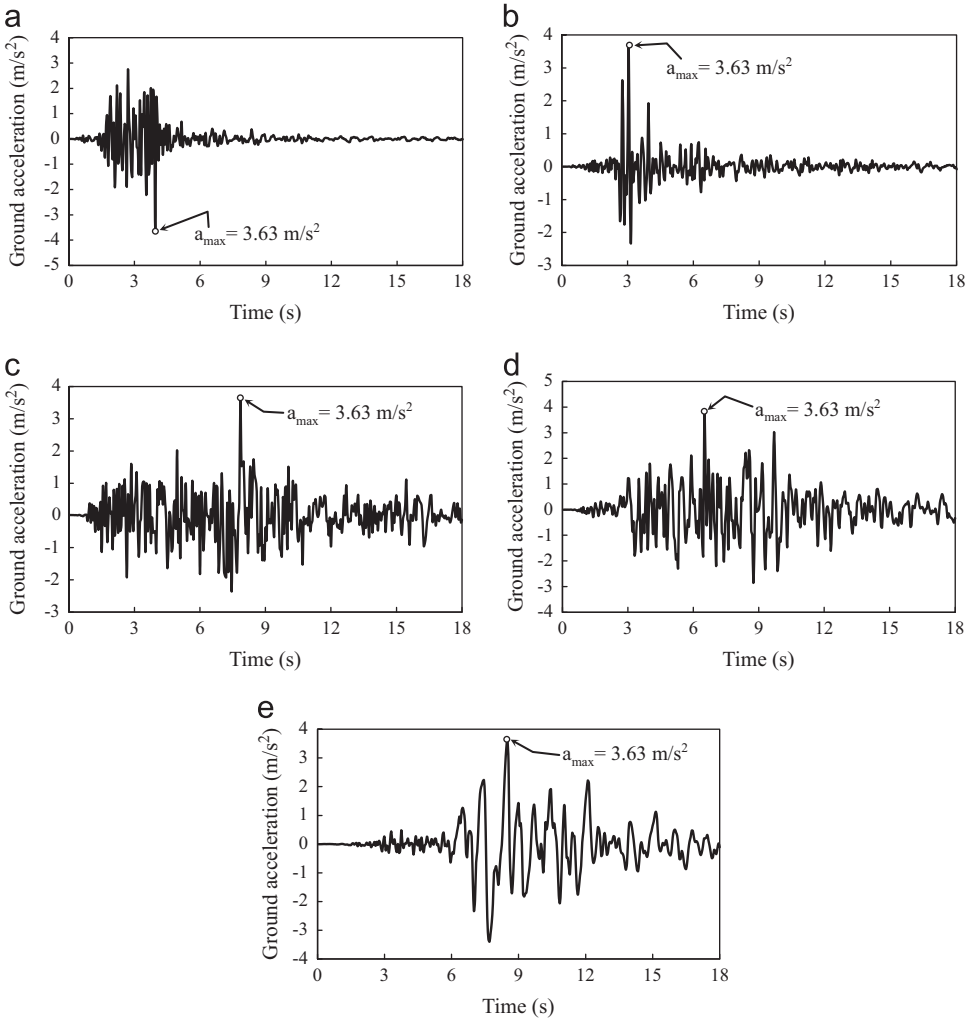

Fig. 10. Scaled horizontal components of earthquake records: (a) 1983 Coalinga (b) 1987 Whittier Narrows (c) 1979 Imperial Valley (d) 1994 Northridge (e) 1989 Loma Prieta.

Table 2
Properties of ground motions considered in this study [75].

Earthquake record	Station	Record/component	Peak ground acceleration (g)	Peak ground velocity (m/s)
1983 Coalinga	1604 Oil City	Coalinga/C-OLC360	0.370	0.124
1987 Whittier Narrows	24400 LA-Obregon Park	Whittier/B-OBR270	0.374	0.145
1979 Imperial Valley	6618 Agrarias	Impvall/H-AGR003	0.370	0.356
1994 Northridge	90053 Canoga Park—Topanga Canyon	Northr/CNP106	0.356	0.321
1989 Loma Prieta	47524 Hollister-South & Pine	Lomap/HSP000	0.371	0.624

Table 3
Properties of soil types considered in this study.

Soil types	E (kN/m^2)	G (kN/m^2)	υ	γ (kg/m^3)	v_s (m/s)	v_p (m/s)
S1	7000,000	2692,308	0.30	2000	1160.24	2170.61
S2	2000,000	769,231	0.30	2000	620.17	1160.24
S3	500,000	185,185	0.35	1900	312.20	649.89
S4	150,000	55,556	0.35	1900	171.00	355.96
S5	75,000	26,786	0.40	1800	121.99	298.81
S6	35,000	12,500	0.40	1800	83.33	204.12

Table 4
Seismic analysis results for Coalinga earthquake.

Maximum responses	Soil types											
	S1		S2		S3		S4		S5		S6	
	t (s)	Value	t (s)	Value	t (s)	Value	t (s)	Value	t (s)	Value	t (s)	Value
u_t (m)	3.9	−0.0002	3.9	0.0002	3.9	0.0014	3.95	0.0045	5.25	0.0078	5.4	0.0132
S_{zb} (MPa)	3.9	0.1728	3.9	−0.1668	2.8	−1.1687	2.8	−2.6230	2.8	−2.7286	2.0	−2.1852
S_{yb} (MPa)	3.9	0.0225	3.9	−0.0221	2.8	−0.1577	2.8	−0.3744	2.8	−0.4041	2.0	−0.3377
S_{xb} (MPa)	3.9	0.0516	3.9	−0.0500	2.8	−0.4176	2.8	−1.0780	2.8	−1.2065	2.0	−1.0772
S_{zf} (MPa)	3.9	−0.1760	3.9	0.1694	2.8	1.1863	2.8	2.6568	2.8	2.7587	2.0	2.2060
S_{yf} (MPa)	3.9	−0.0153	3.9	0.0154	2.8	0.1032	2.8	0.2330	2.8	0.2472	2.0	0.1975
S_{xf} (MPa)	3.9	−0.0258	3.9	0.0242	2.8	0.1410	2.8	0.2601	2.8	0.2455	2.0	0.1471

u_t: Maximum lateral top displacement of cantilever wall; S_{zb}, S_{yb} and S_{xb}: Maximum stresses estimated on the back face (backfill side) of the cantilever wall in z, y and x directions, respectively; S_{zf}, S_{yf} and S_{xf}: Maximum stresses estimated on the front face of the cantilever wall in z, y and x directions, respectively.

is considered as low frequency ground motion, the Imperial Valley and Northridge records are categorized as intermediate frequency excitations, and the Coalinga and Whittier Narrows records are taken into account as high frequency content excitations. It should not be forgotten here that the PGV/PGA or PGA/PGV ratio is a very important parameter to characterize the damage potential of near-fault ground motions and indicated as being a measure of destructiveness [76]. The ground motions with higher PGV/PGA values have larger damage potential [77,78].

To evaluate the variation of the dynamic response of cantilever retaining wall supported on flexible foundation, six soil types are considered in the analyzes. The foundation soil properties are shown in Table 3. In the finite element analyzes, the Young's Modulus, the Poisson's ratio, the unit weight and the internal friction angle of cohesionless backfill soil are taken to be 30 MPa, 0.35, 18 kN/m^3 and 30°, respectively. Furthermore, Rayleigh damping is taken into consideration in the seismic analyzes. The damping values for both structure and soil are also taken as 5%.

7. Results and discussions

Results, obtained by applying the proposed methodology, are presented in terms of the lateral displacements and stresses in two parts. In the first part, a detailed discussion on the effects of soil–structure interaction on seismic behavior of cantilever wall is given. In the second part, the effects of earthquake frequency content on dynamic behavior of cantilever wall subjected to the combined effects of backfill and soil/foundation interactions are discussed. Tables 4–8 report the peak responses and the corresponding times calculated for varying the soil types and the ground motions. The tables clearly indicate the effects of soil–structure interaction and earthquake frequency content so that the maximum values of both lateral displacements and stresses changed significantly. These effects on seismic response of cantilever wall are shown graphically, and discussed comparatively below. It is important to note here that since all results obtained from the analyzes cannot be illustrated, some comparisons were selected to describe the system behavior.

7.1. Effects of soil–structure interaction

Fig. 11 shows the height-wise variations of the lateral displacements of cantilever retaining wall for varying the foundation soil conditions under the effects of three different ground motions. It is worth noting here that these displacements represent the relative lateral displacements of the wall with respect to the ground. While the negative displacements refer to the movements away from the backfill, the positive ones refer to the movements toward the backfill. It is observed from this figure that as the soil stiffness decreases, the displacement response

Table 5
Seismic analysis results for Whittier Narrows earthquake.

Maximum responses	Soil types											
	S1		S2		S3		S4		S5		S6	
	t (s)	Value	t (s)	Value	t (s)	Value	t (s)	Value	t (s)	Value	t (s)	Value
u_t (m)	3.1	−0.0002	3.1	0.0002	3.1	0.0015	3.15	0.0036	3.15	0.0050	3.15	0.0048
S_{zb} (MPa)	3.1	0.2169	3.1	−0.2114	3.1	−1.5835	3.1	−3.2310	3.1	−3.1689	3.15	−2.5386
S_{yb} (MPa)	3.1	0.0284	3.1	−0.0281	3.1	−0.2182	3.1	−0.4685	3.1	−0.4753	3.15	−0.3940
S_{xb} (MPa)	3.1	0.0625	3.1	−0.0608	3.1	−0.5613	3.1	−1.3301	3.1	−1.4046	3.15	−1.2561
S_{zf} (MPa)	3.1	−0.2211	3.1	0.2149	3.1	1.6076	3.1	3.2719	3.1	3.2022	3.15	2.5650
S_{yf} (MPa)	3.1	−0.0197	3.1	0.0200	3.1	0.1450	3.1	0.2942	3.1	0.2925	3.15	0.2308
S_{xf} (MPa)	3.1	−0.0345	3.1	0.0334	3.1	0.2095	3.1	0.3424	3.1	0.3007	3.15	0.1735

Table 6
Seismic analysis results for Imperial Valley earthquake.

Maximum responses	Soil types											
	S1		S2		S3		S4		S5		S6	
	t (s)	Value	t (s)	Value	t (s)	Value	t (s)	Value	t (s)	Value	t (s)	Value
u_t (m)	7.75	0.0007	7.75	−0.0008	7.75	−0.0055	7.8	−0.0155	7.8	−0.0238	7.85	−0.0340
S_{zb} (MPa)	7.75	−0.4410	7.75	0.4471	7.75	3.0657	7.75	6.2592	7.75	6.7292	8.05	−5.9313
S_{yb} (MPa)	7.75	−0.0531	7.75	0.0545	7.75	0.3877	7.75	0.8205	7.75	0.9112	8.05	−0.8975
S_{xb} (MPa)	7.75	−0.1301	7.75	0.1428	7.75	1.1218	7.75	2.4733	7.75	2.8154	8.05	−2.7691
S_{zf} (MPa)	7.75	0.4487	7.75	−0.4539	7.75	−3.1081	7.75	−6.3392	7.75	−6.8060	8.05	5.9748
S_{yf} (MPa)	7.75	0.0359	7.75	−0.0357	7.75	−0.2397	7.75	−0.4933	7.75	−0.5423	8.05	0.5352
S_{xf} (MPa)	7.75	0.0555	7.75	−0.0472	7.75	−0.2534	7.75	−0.4530	8.0	0.4804	8.05	0.3961

Table 7
Seismic analysis results for Northridge earthquake.

Maximum responses	Soil types											
	S1		S2		S3		S4		S5		S6	
	t (s)	Value	t (s)	Value	t (s)	Value	t (s)	Value	t (s)	Value	t (s)	Value
u_t (m)	8.65	−0.0005	8.65	0.0005	8.65	0.0044	8.65	0.0125	8.7	0.0191	8.75	0.0238
S_{zb} (MPa)	8.6	0.4367	8.65	−0.3194	8.6	−2.7645	8.65	−7.3157	8.65	−9.1277	8.65	−8.3339
S_{yb} (MPa)	8.6	0.0549	8.65	−0.0386	8.6	−0.3587	8.65	−0.9750	8.65	−1.2572	8.65	−1.1969
S_{xb} (MPa)	8.6	0.1232	8.65	−0.0882	8.65	−0.9968	8.65	−2.9641	8.65	−3.8864	8.65	−3.8803
S_{zf} (MPa)	8.6	−0.4449	8.65	0.3250	8.6	2.8049	8.65	7.4092	8.65	9.2351	8.65	8.4191
S_{yf} (MPa)	8.6	−0.0382	8.65	0.0272	8.6	0.2294	8.65	0.5834	8.65	0.7487	8.65	0.6939
S_{xf} (MPa)	8.6	−0.0654	8.6	0.0474	8.6	0.2904	8.6	0.5562	8.65	0.6353	8.65	0.5219

Table 8
Seismic analysis results for Loma Prieta earthquake.

Maximum responses	Soil types											
	S1		S2		S3		S4		S5		S6	
	t (s)	Value	t (s)	Value	t (s)	Value	t (s)	Value	t (s)	Value	t (s)	Value
u_t (m)	8.2	0.0009	8.2	−0.0010	8.2	−0.0075	8.25	−0.0219	8.3	−0.0343	8.3	−0.0523
S_{zb} (MPa)	8.15	−0.5479	8.15	0.5592	7.9	3.9685	7.9	10.1317	7.9	13.1700	7.9	12.5971
S_{yb} (MPa)	7.85	−0.0676	8.15	0.0673	7.85	0.5199	7.85	1.3618	7.9	1.8017	7.9	1.8326
S_{xb} (MPa)	8.15	−0.1542	8.15	0.1727	7.9	1.4700	7.9	4.1134	7.9	5.6318	7.9	5.9426
S_{zf} (MPa)	8.15	0.5578	8.15	−0.5682	7.9	−4.0262	7.9	−10.2604	7.9	−13.3271	7.9	−12.7250
S_{yf} (MPa)	7.85	0.0479	7.85	−0.0472	7.85	−0.3355	7.85	−0.8235	7.9	−1.0731	7.9	−1.0664
S_{xf} (MPa)	7.85	0.0860	7.85	−0.0837	7.8	−0.4408	7.85	−0.8218	7.85	−0.9809	7.9	−0.8062

generally increases for all ground motions, and this reflects a significant soil–structure interaction influence on the response.

It is possible to evaluate the lateral displacements in terms of time history using the suggested model. Accordingly, the deviations of the displacements in time are illustrated and compared in Fig. 12 in order to clarify the changes of the lateral top displacement values due to the flexible foundation conditions. It can be noted from Fig. 12 that the response amplification/reduction has occurred

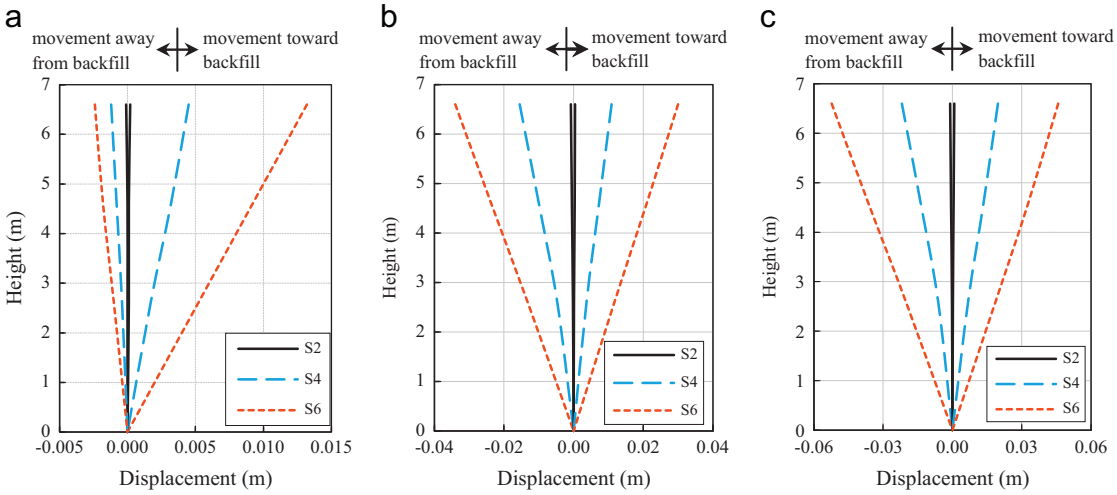

Fig. 11. Calculated lateral displacements along the height of the cantilever wall for (a) Coalinga (b) Imperial Valley (c) Loma Prieta earthquakes.

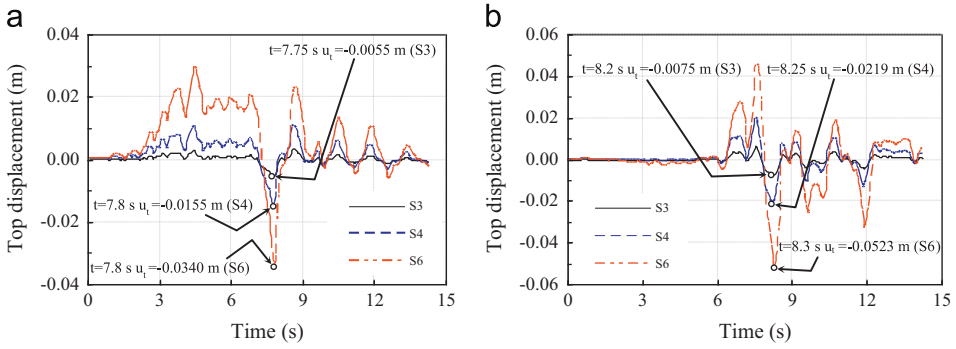

Fig. 12. Time histories of lateral top displacement of the cantilever retaining wall for (a) Imperial Valley (b) Loma Prieta earthquakes.

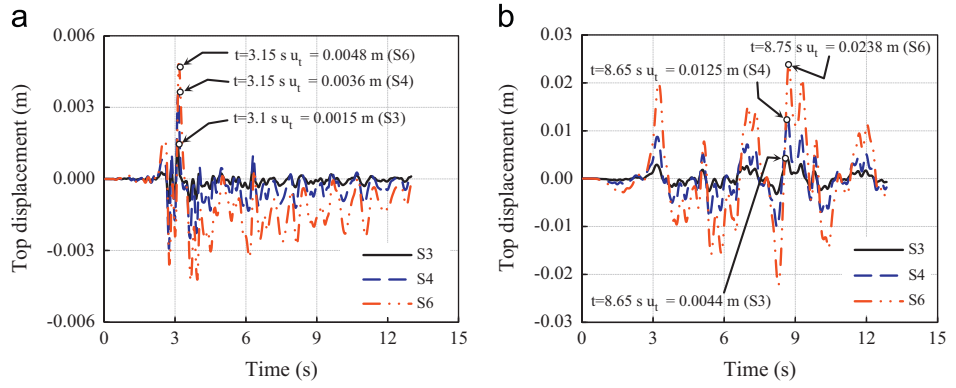

Fig. 13. Time histories of lateral top displacement of the cantilever retaining wall for (a) Whittier Narrows (b) Northridge earthquakes.

depending on the soil/foundation conditions. For example, while the maximum lateral displacement is estimated as 0.0055 m for S3 soil type, the same quantity is calculated as 0.0340 m for S6 soil type in case of Imperial Valley earthquake. Thus, it can be highlighted that soil–structure interaction affects the system behavior so that the dramatic increment in the displacement response is almost at a level of 519% between S3 and S6 soil types. A similar trend is observed for Loma Prieta earthquake as well, the maximum displacement responses due to the soil–structure interaction are highly magnified, and the responses tend to increase with decreasing soil stiffness. For instance, the value of peak lateral displacement is 0.0075 m for S3 soil type, whereas the displacements are computed as 0.0219 m and 0.0523 m for S4 and S6 soil types, respectively. It is obvious that soil–structure interaction leads to the dramatic increments of about 192% and 597% in peak displacement responses for S4 and S6 soil types in comparison with S3 soil type, respectively. If similar comparisons are also made for Whittier Narrows and Northridge earthquakes from Fig. 13, same tendency can be observed. These variations reveal a significant soil–structure interaction effect on the response, and confirm that the exclusion of the accurate soil properties may cause underestimation or overestimation of the displacement response, and this, in turn, fairly affects the design process due to the displacement sensitivity of cantilever retaining walls.

The estimated stress responses and their variations in time at the back and the front faces of the cantilever retaining wall can be compared with each other to introduce the soil–structure

interaction effects. Under the effect of Coalinga earthquake, the comparisons of stress time history responses in z and x directions for both back and front faces of the cantilever wall are shown in Figs. 14 and 15, respectively. As these figures depict, the maximum stresses obtained at the critical sections of the wall change with varying soil conditions. For example, at the back face of the wall in z direction, while the peak stress, as compression, has the value of 1.1687 MPa for S3 soil type, it is calculated as 2.7286 MPa for S5 soil type. This reflects a stress increment of about 133% between S3 and S5 soil types due to the variation of soil conditions. A similar trend can be observed at the front face of the wall as well, the maximum stress responses due to the soil–structure interaction are highly magnified (see Fig. 14b). For instance, the value of peak stress is 0.1760 MPa for S1 soil type, whereas the same quantity is calculated as 1.1863 MPa for S3 soil type, and a stress increment of nearly 574% takes place at the front face of the wall. Furthermore, it is important to state here that the peak responses of stresses in the wall in z direction take place at the level of 0.2 m from the top of the foundation. If similar comparisons are made in x direction as seen in Fig. 15, the same trend and soil–structure interaction effects can be clearly observed. For example, the changing of soil type from S3 to S5 causes a stress increment of about 189% at the back face of the wall. Furthermore, as can be seen from Fig. 15, the maximum responses at back and front faces of the wall differ remarkably.

When the computations are carried out for the systems under the effects of Imperial Valley and Loma Prieta earthquakes as seen in Figs. 16 and 17, it is possible to observe the soil–structure interaction effects once again. The most important point arising

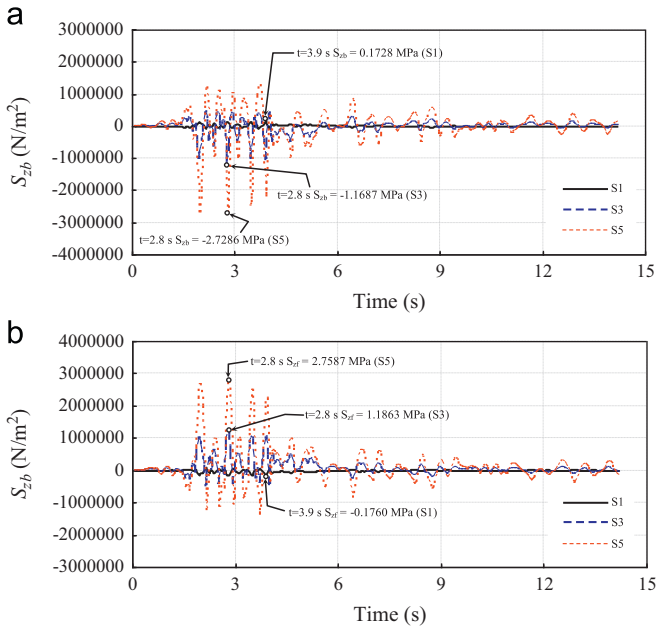

Fig. 14. Time histories of stress in z direction at (a) back face (b) front face of the cantilever wall for Coalinga earthquake.

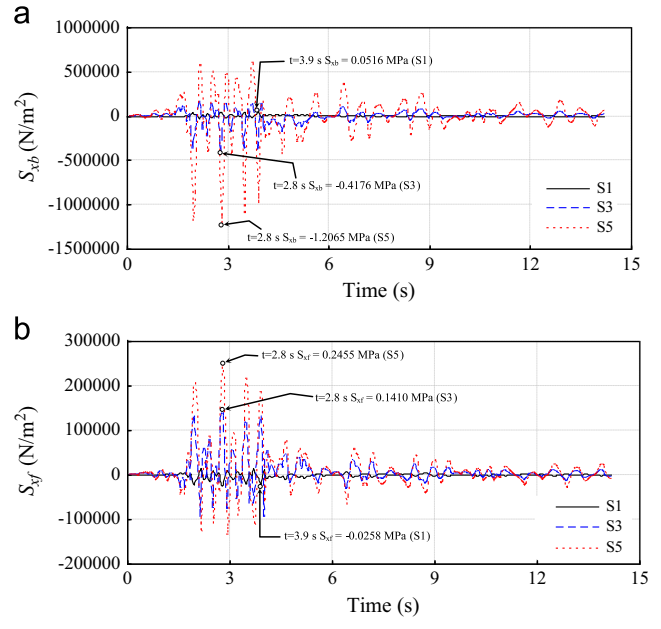

Fig. 15. Time histories of stress in x direction at (a) back face (b) front face of the cantilever wall for Coalinga earthquake.

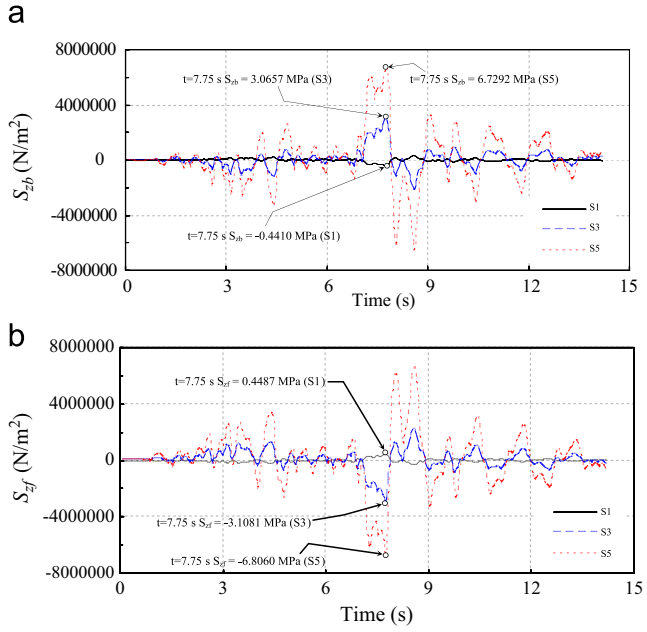

Fig. 16. Time histories of stress in z direction at (a) back face (b) front face of the cantilever wall for Imperial Valley earthquake.

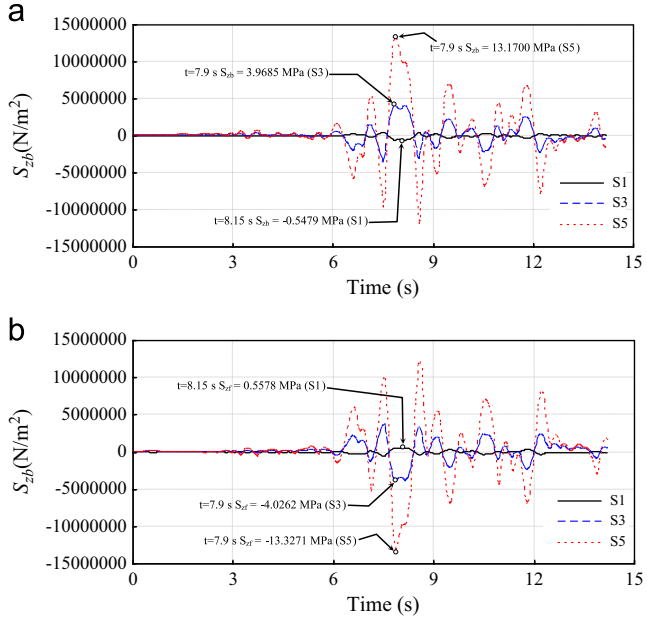

Fig. 17. Time histories of stress in z direction at (a) back face (b) front face of the cantilever wall for Loma Prieta earthquake.

from these comparisons is that the variation of the soil properties notably affects the stress response of the system. This implies that the response amplification or reduction pattern due to the deformable foundation is highly dependent on the soil properties, and the time history diagrams describe different behaviors of the structure for all ground motions. Therefore, these evaluations should be considered as an alert that especially the mechanical properties of soil are extremely sensitive parameters affecting the results and thus should be measured with utmost care.

7.2. Effects of earthquake frequency content

In fact, the previous evaluations and comparisons clearly show the effects of earthquake frequency content on dynamic response of cantilever retaining wall. Accordingly, Tables 4–8 indicate that effect of earthquake frequency content is significant on the structural response of the wall so that the peak responses are different from each other depending on the variation of the ground motion. Another sign of the frequency content influence on the response is that the occurrence times of response change with changing earthquake record. Furthermore, all maximum responses increase as the frequency content of the considered earthquakes decreases, and this is valid for all soil types. At this point, this can be attributed to the magnitudes of the considered earthquakes since the Coalinga earthquake had a magnitude of 5.2, the Whittier Narrows earthquake had a magnitude of 5.3, the Imperial Valley earthquake had a magnitude of 6.5, the Northridge earthquake had a magnitude of 6.7 and the Loma Prieta earthquake had a magnitude of 6.9. The effects of the frequency content on seismic response of the cantilever wall are illustrated, and their implications are also discussed comprehensively below.

A comparison among the height-wise variations of lateral displacements of cantilever wall under earthquake effects with different frequency contents is presented in Fig. 18. It is worth noting once again that these displacements represent the relative lateral displacements of the wall with respect to the ground. Effects of earthquake frequency content on the displacement response of the wall are clearly observed from this figure, and it is obvious that the structural response is highly dependent on the earthquake frequency content so that a considerable increase occurs in displacement response due to the frequency content variation. The results show that the responses due to low frequency content earthquake of Loma Prieta are highly magnified, and the least response values are obtained under the Coalinga and Whittier Narrows earthquakes with high frequency content.

To clarify the changes of the lateral displacement due to different earthquake records, the deviations of the displacements in time are illustrated and compared for S3 and S6 soil types in Fig. 19. As Fig. 19a demonstrates, while the maximum lateral top displacement is calculated as 0.0055 m at 7.75 s for Imperial Valley earthquake with moderate frequency content, the same quantity is computed as 0.0075 m at 8.2 s for Loma Prieta earthquake with low frequency content. Hence, it can be noted that input earthquake motion affects the system behavior so that the increment in the displacement response is almost at a level of 37%. If similar comparison is made for S6 soil type, a similar trend of an increase in the response can be seen (see Tables 4–8). For instance, the value of maximum lateral displacement is 0.0132 m for Coalinga earthquake, while the displacements are estimated as 0.0340 m and 0.0523 m for Imperial Valley and Loma Prieta earthquakes, respectively. It is clear that the variation of the ground motion leads to the dramatic increments of about 158% and 296% in peak displacement responses for Imperial Valley and Loma Prieta earthquakes compared to the Coalinga record, respectively. When the calculations are carried out for the systems under the effects of Whittier Narrows and Northridge earthquakes as seen in Fig. 20, it is possible to observe the earthquake frequency content effects once again. It is found that the effect of earthquake frequency content is quite significant on the displacement response, and may cause a considerable increase in time domain peak response values.

In addition to the lateral displacement response, stress behavior of the cantilever wall is thoroughly investigated in this section. The time history diagrams of stress responses at the back face of the cantilever retaining wall in z and x directions for S3 and S6 soil types are presented in Figs. 21 and 22, depending on the five different ground motions. As these figures depict, the maximum stress responses obtained at the critical sections of the wall generally tend to increase in absolute value with decrement in the frequency content. For example, at the back face of the wall in z direction for S3 soil type, while the maximum stress, as compression, has the value of 1.1687 MPa for Coalinga record

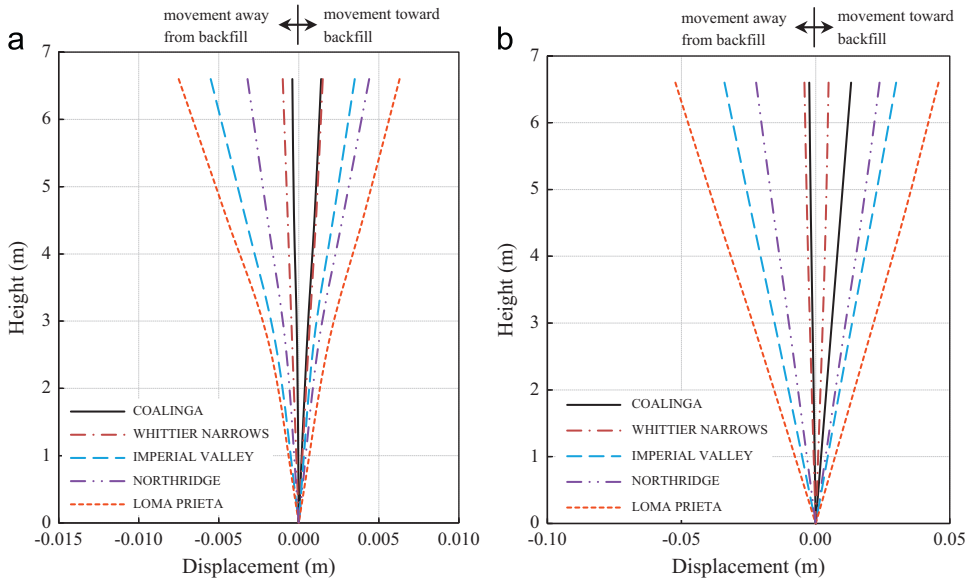

Fig. 18. Comparison of the lateral displacements of the cantilever wall under the effect of five different ground motions for (a) S3 (b) S6 soil types.

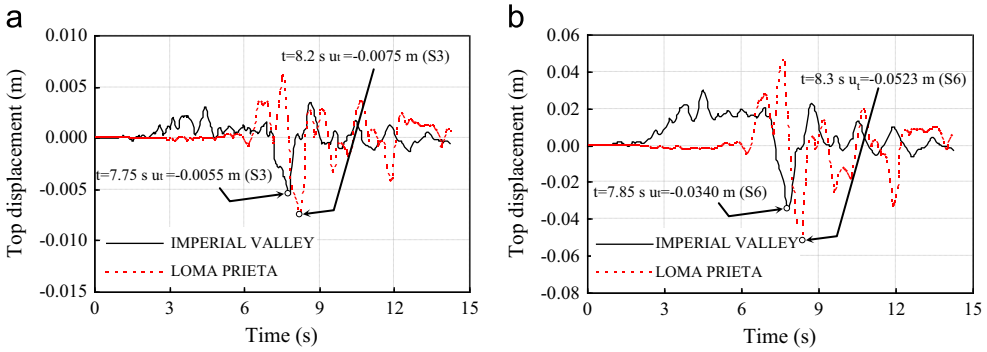

Fig. 19. Variation of lateral displacements in time under the effect of Imperial Valley and Loma Prieta earthquakes for (a) S3 (b) S6 soil types.

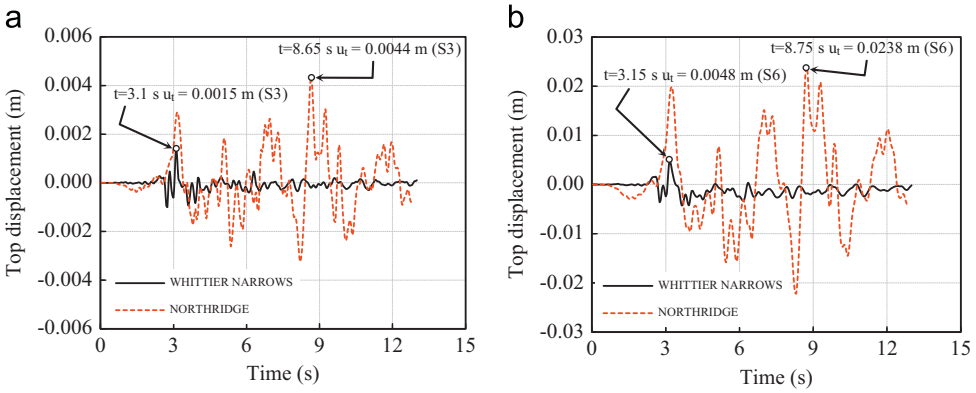

Fig. 20. Variation of lateral displacements in time under the effect of Whittier Narrows and Northridge earthquakes for (a) S3 (b) S6 soil types.

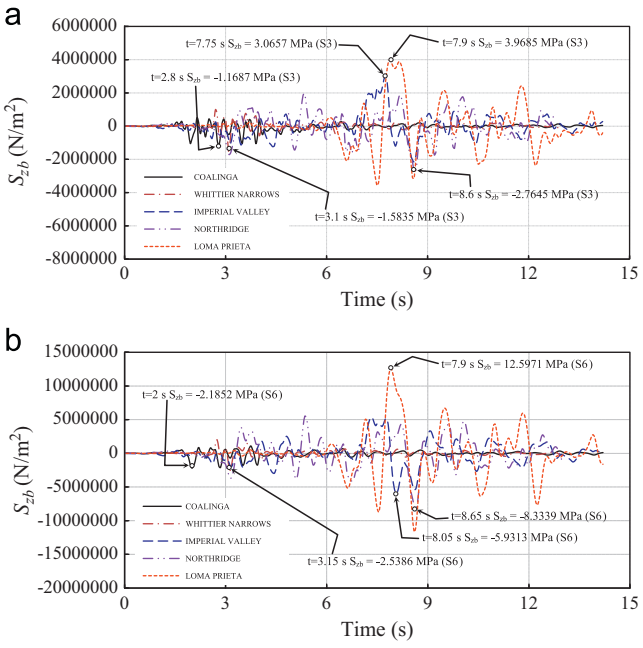

Fig. 21. Variation of stresses in z direction at the back face of the cantilever wall under the effect of five different ground motions for (a) S3 (b) S6 soil types.

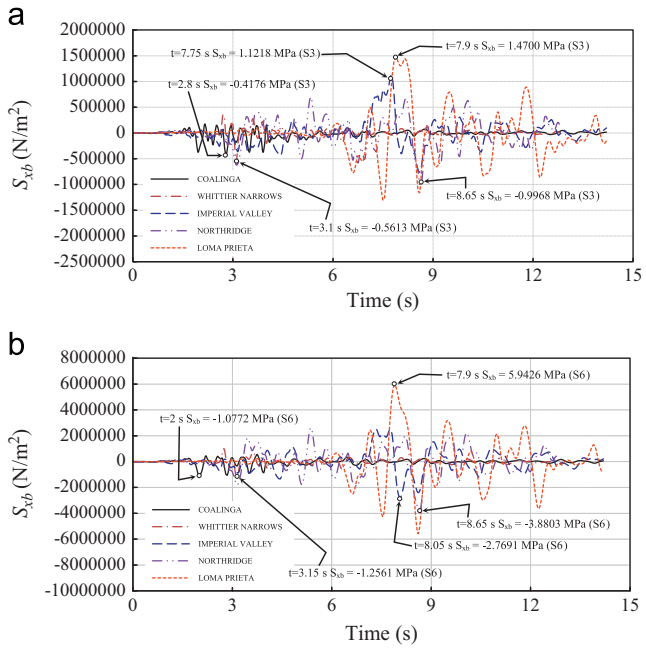

Fig. 22. Variation of stresses in x direction at the back face of the cantilever wall under the effect of five different ground motions for (a) S3 (b) S6 soil types.

with high frequency content, its value is 3.9685 MPa for Loma Prieta earthquake with low frequency content, as tension. This reflects an increase of about 239% in stress value due to the variation of the ground motion. The same tendency can be observed for S6 soil type, as seen in Fig. 21b. For instance, the value of peak stress is 2.1852 MPa under the Coalinga record, whereas the same quantity is calculated as 12.5971 MPa under the Loma Prieta earthquake, and a dramatic stress increment of approximately 476% occurs. This implies that the effect of earthquake frequency content on seismic response of cantilever walls is more pronounced for relatively soft soil conditions (like S5 and S6).

If similar comparisons are carried out in x direction at the back face of the cantilever wall as seen in Fig. 22, it is clearly observed

that the response amplification has occurred for all cases as the input earthquake changes. For example, in S6 soil type, the peak stress is 1.2561 MPa for high frequency content record of Whittier Narrows, it is calculated as 3.8803 MPa for moderate frequency content record of Northridge, and it is 5.9426 MPa for low frequency content earthquake of Loma Prieta. This comparison reveals frequency content effects on seismic response once again.

It is clear that the response amplification or reduction pattern due to deformable foundation is highly dependent on the nature of the earthquake.

8. Conclusions

A seismic analysis procedure that can be used for the determination of dynamic behavior of cantilever retaining walls under horizontal ground excitation in three-dimensional space is presented in this study. The study explores different factors such as soil–structure interaction and earthquake frequency content which may have considerable effect on the seismic response of cantilever walls. The soil is modeled as an elasto-plastic medium obeying the Drucker–Prager yield criterion, and backfill–wall interface behavior is taken into account by using interface elements between the wall and soil to allow for de-bonding. Viscous boundary model is also used to simulate the wave energy absorption.

Five different ground motions with same peak ground acceleration are applied to examine the effect of earthquake frequency content on the seismic behavior of backfill–cantilever wall–soil/foundation interaction system. The effect of foundation deformability on the overall seismic response of the system is also investigated by comparing the results among six different soil types under five different earthquake records.

The computational results include the lateral displacements and stresses in the wall obtained from nonlinear time history analyzes of the considered system. It is found that soil–structure interaction has a significant effect on the seismic behavior of cantilever wall. Therefore, the exclusion of the accurate soil properties may cause underestimation or overestimation of the response, and this, in turn, may lead to unsafe seismic design of R/C cantilever retaining walls.

The earthquake frequency content may also be one of the most important parameters to be considered in seismic analysis and design. In general, as the soil gets softer, the earthquake frequency content becomes more effective, and affects the system behavior more. This conclusion is valid for almost all response parameters investigated in this study, namely the lateral displacement over the height of the structure, top displacement and stress. Furthermore, it is found that the ground motions with higher PGV/PGA values have larger damage potential on cantilever retaining walls.

It is clear that the dynamic behavior of cantilever walls depends on a wide range of parameters such as nature of earthquakes, backfill interaction and soil/foundation interaction which should be taken into consideration in current codes of practice. Accordingly, this research provides an important addition to the available knowledge database of the seismic analysis of cantilever walls.

References

[1] Li X, Wu Y, He S. Seismic stability analysis of gravity retaining walls. Soil Dynamics and Earthquake Engineering 2010;30:875–8.
[2] Ling HI, Leshchinsky D. Chou NNS. Post-earthquake investigation on several geosynthetic-reinforced soil retaining walls and slopes during the Ji–Ji earthquake of Taiwan. Soil Dynamics and Earthquake Engineering 2001;21:297–313.
[3] Trandafir AC, Kamai T, Sidle RC. Earthquake-induced displacements of gravity retaining walls and anchor-reinforced slopes. Soil Dynamics and Earthquake Engineering 2009;29:428–37.
[4] Han Q, Du X, Liu J, Li Z, Li L, Zhao J. Seismic damage of highway bridges during the 2008 Wenchuan earthquake. Earthquake Engineering and Engineering Vibration 2009;8(2):263–73.
[5] Veletsos AS, Younan AH. Dynamic soil pressures on rigid vertical walls. Earthquake Engineering and Structural Dynamics 1994;23(3):275–301.
[6] Mononobe N, Matsuo H. On the determination of earth pressures during earthquakes. Proceedings of world engineering congress: Japan; 1929. 9, , p. 179–87.
[7] Okabe S. General theory of earth pressure and seismic stability of retaining wall and dam. Journal of Japanese Society of Civil Engineering 1924;10(6):1277–323.
[8] Seed HB, Whitman RV. Design of earth retaining structures for dynamic loads. Proceedings of the Speciality Conference on Lateral stresses in the ground and design of earth retaining structures. ASCE, Ithaca: New York; 1970. pp.103–47.
[9] Richards R, Elms DG. Seismic behavior of gravity retaining walls. ASCE Journal of the Geotechnical Engineering Division 1979;105:449–64.
[10] Nadim F, Whitman RV. Seismically induced movement of retaining walls. ASCE Journal of the Geotechnical Engineering Division 1983;109(7):915–31.
[11] ATC. Seismic design guidelines for highway bridges. ATC-6, Palo Alto: CA; 1981.
[12] EC-8. Design provisions for earthquake resistance of structures. Part 5; 1994.
[13] Matsuo H, Ohara S. Lateral earth pressure and stability of quay walls during earthquakes. Proceedings of 2nd world conference on earthquake engineering; 1960. 1, p.165–81.
[14] Wood JH. Earthquake-induced soil pressures on structures. Report EERL 73-05, earthquake engineering research laboratory, California Institute of Technology; 1973.
[15] Wood JH. Earthquake-induced pressures on rigid wall structure. Bulletin of New Zeeland Society of Earthquake Engineering 1975;8:175–86.
[16] Arias A, Sanchez-Sesma FJ, Ovando-Shelley E. A simplified elastic model for seismic analysis of earth-retaining structures with limited displacement. Proc. of international conference on recent advances in geotechnical earthquake engineering and soil dynamics. St. Louis: MO; April 1981. I, p. 235–240.
[17] Veletsos AS, Younan AH. Dynamic modeling and response of soil–wall systems. ASCE Journal of Geotechnical Engineering 1994;120(12):2155–79.
[18] Veletsos AS, Younan AH. Dynamic soil pressures on vertical walls. In: S. Prakash, editor. Proceedings of third international conference on recent advances in geotechnical earthquake engineering and soil dynamics, Vol. III. Rolla, MO: University of Missouri; 1995. p. 1589–1604.
[19] Veletsos AS, Younan AH. Dynamic response of cantilever walls. ASCE Journal of Geotechnical Engineering 1997;123(2):161–72.
[20] Younan AH, Veletsos AS. Dynamic response of flexible retaining walls. Earthquake Engineering and Structural Dynamics 2000;29:1815–44.
[21] Giarlelis C, Mylonakis G. Interpretation of dynamic retaining wall model tests in light of elastic and plastic solutions. Soil Dynamics and Earthquake Engineering 2011;31:16–24.
[22] Theodorakopoulos DD, Chassiakos AP, Beskos DE. Dynamic pressures on rigid cantilever walls retaining poroelastic soil media. Part I. First method of solution. Soil Dynamics and Earthquake Engineering 2001;21:315–38.
[23] Siddharthan R, Norris GM, Maragakis EA. Deformation response of rigid retaining walls to seismic excitation. In: Cakmak AS, Herrera I, editors. Structural dynamics and soil–structure interaction. Southampton: CMP; 1989. p. 315–30.
[24] Siller TJ, Christiano PP, Bielak J. Seismic response of tied-back retaining walls. Earthquake Engineering and Structural Dynamics 1991;20:605–20.
[25] Elgamal AW, Alampalli S. Earthquake response of retaining walls:full scale testing and computational analysis. In: Proceedings of 10th world conference on earthquake engineering, Madrid, Spain. AA Rotterdam: Balkema, 3; 1992. pp. 1671–76.
[26] Al-Homoud AS, Whitman RV. Evaluating tilt of gravity retaining walls during earthquakes. In: Proceedings of 10th world conference on earthquake engineering, Madrid, Spain. AA Rotterdam: Balkema, 3; 1992. p. 1683–1688.
[27] Al-Homoud AS, Whitman RV. Seismic analysis and design of rigid bridge abutments considering rotation and sliding incorporating non-linear soil behavior. Soil Dynamics and Earthquake Engineering 1999;18:247–77.
[28] Wu G, Finn WDL. Seismic lateral pressures for design of rigid walls. Canadian Geotechnical Journal 1999;36:509–22.
[29] Psarropoulos PN, Klonaris G, Gazetas G. Seismic earth pressures on rigid and flexible retaining walls. Soil Dynamics and Earthquake Engineering 2005;25: 795–809.
[30] Theodorakopoulos DD, Chassiakos AP, Beskos DE. Dynamic pressures on rigid cantilever walls retaining poroelastic soil media. Part II. Second method of solution. Soil Dynamics and Earthquake Engineering 2001;21:339–64.
[31] Theodorakopoulos DD. Dynamic pressures on a pair of rigid walls retaining poroelastic soil. Soil Dynamics and Earthquake Engineering 2003;23:41–51.
[32] Lanzoni L, Radi E, Tralli A. On the seismic response of a flexible wall retaining a viscous poroelastic soil. Soil Dynamics and Earthquake Engineering 2007;27:818–42.
[33] Elgamal AW, Alampalli S, Laak PV. Forced vibration of full-scale wall–backfill system. ASCE Journal of Geotechnical Engineering 1996;122(10):849–58.
[34] Madabhushi SPG, Zeng X. Simulating seismic response of cantilever retaining walls. ASCE Journal of Geotechnical and Geoenvironmental Engineering 2007;133:539–49.

[35] Mylonakis G, Kloukinas P, Papantonopoulos C. An alternative to the Mononobe–Okabe equations for seismic earth pressures. Soil Dynamics and Earthquake Engineering 2007;27:957–69.
[36] Evangelista A, di Santolo AS, Simonelli AL. Evaluation of pseudostatic active earth pressure coefficient of cantilever retaining walls. Soil Dynamics and Earthquake Engineering 2010;30:1119–28.
[37] Stamos AA, Beskos DE. 3-D seismic response analysis of long lined tunnels in half-space. Soil Dynamics and Earthquake Engineering 1996;15:111–8.
[38] Hatzigeorgiou GD, Beskos DE. Soil–structure interaction effects on seismic inelastic analysis of 3-D tunnels. Soil Dynamics and Earthquake Engineering 2010;30(9):851–61.
[39] Cakir T, Livaoglu R. Fast practical analytical model for analysis of backfill-rectangular tank-fluid interaction systems. Soil Dynamics and Earthquake Engineering 2012;37:24–37.
[40] Turkish Earthquake Code (TEC). Specification for structures to be built in disaster areas. Ministry of Public Works and Settlement Government of Republic of Turkey; 2007.
[41] IS 1893. Indian standard criteria for earthquake for earthquake resistant design of structures. Part 1, General provisions and buildings; 2002.
[42] EC-8. Design of structures for earthquake resistance—part 5: Foundations, retaining structures and geotechnical aspects. Final draft, European Committee for Standardization, Brussels: Belgium; December 2003.
[43] Kramer SL. Geotechnical earthquake engineering. New Jersey: Prentice-Hall; 1996.
[44] Kermani E, Jafarian Y, Baziar MH. New predictive models for the v_{max}/a_{max} ratio of strong ground motions using genetic programming. International Journal of Civil Engineering 2009;7(4):236–47.
[45] Newmark NM. A study of vertical and horizontal earthquake spectra. NM newmark consulting engineering services. Directorate of licencing, US atomic energy comission: Washington, DC; 1973.
[46] McGuire RK. Seismic ground motion parameter relations. ASCE Journal of the Geotechnical Engineering Division 1978;104(GT4):481–90.
[47] Tso WK, Zhu TJ, Heidebrecht AC. Engineering implications of ground motion A/V ratio. Soil Dynamics and Earthquake Engineering 1992;11(3):133–44.
[48] Kianoush MR, Ghaemmaghami AR. The effect of earthquake frequency content on the seismic behavior of concrete rectangular liquid tanks using the finite element method incorporating soil–structure interaction. Engineering Structures 2011;33:2186–200.
[49] Pitilakis D, Dietz M, Wood DM, Clouteau D, Modaressi A. Numerical simulation of dynamic soil–structure interaction in shaking table testing. Soil Dynamics and Earthquake Engineering 2008;28(6):453–67.
[50] ANSYS. ANSYS Inc., Canonsburg, PA; 2006.
[51] Wolf JP, Song C. Some cornerstones of dynamic soil–structure interaction. Engineering Structures 2002;24:13–28.
[52] Wolf JP. Foundation vibration analysis using simple physical models. New Jersey: Prentice-Hall; 1994.
[53] Luco JE, Hadjian AH. Two-dimensional approximations to the three-dimensional soil–structure interaction problem. Nuclear Engineering and Design 1974;31:195–203.
[54] Wolf JP, Song C. Finite element modeling of unbounded media. 11th world conference on earthquake engineering. San Francisco; 1996. p.1–8.
[55] Lysmer J, Kuhlemeyer RL. Finite dynamic model for infinite media. ASCE Journal of the Engineering Mechanics Division 1969;95:859–77.
[56] Kuhlemeyer RL, Lysmer J. Finite element method accuracy for wave propagation problems. ASCE Journal of the Soil Mechenics and Foundation Division 1973;99:421–7.
[57] Clayton J, Enquist B. Absorbing boundary conditions for acoustic and elastic wave equations. Bulletin of the Seismological Society of America 1977;67:1529–41.
[58] Liao ZP, Wong HL. A transmitting boundary for the numerical simulation of elastic wave propagation. Soil Dynamics and Earthquake Engineering 1984;3(4):174–83.
[59] Navarro C, Samartin A. Dynamic earth pressures against a retaining wall caused by Rayleigh waves. Engineering Structures 1989;11:31–6.
[60] Song C, Wolf JP. Dynamic stiffness of unbounded medium based on solvent damping extraction method. Earthquake Engineering and Structural Dynamics 1994;23:1073–86.
[61] Wolf JP, Song C. Doubly asymptotic multi-directional transmitting boundary for dynamic unbounded medium–structure–interaction analysis. Earthquake Engineering and Structural Dynamics 1995;24:175–88.
[62] Wolf JP, Song C. Finite element modeling of unbounded media. Chichester: John Wiley&Sons; 1996.
[63] Nofal EMH. Analysis of non-linear soil–pile interaction under dynamic lateral loading. PhD Thesis, University of California, Irvine; 1998.
[64] Zerfa Z, Loret B. A viscous boundary for transient analyses of saturated porous media. Earthquake Engineering and Structural Dynamics 2004;33:89–110.
[65] Livaoglu R, Dogangun A. Effect of foundation embedment on seismic behavior of elevated tanks considering fluid–structure–soil interaction. Soil Dynamics and Earthquake Engineering 2007;27:855–63.
[66] Livaoglu R, Cakir T, Dogangun A, Aytekin M. Effects of backfill on seismic behavior of rectangular tanks. Ocean Engineering 2011;38:1161–73.
[67] Wilson EL. Three-dimensional static and dynamic analysis of structures—a physical approach with emphasis on earthquake engineering. Berkeley, California, USA: Computers and Structures, Inc.; 2002.
[68] Wolf JP. Spring–dashpot–mass models for foundation vibrations. Earthquake Engineering and Structural Dynamics 1997;26:931–49.
[69] Chopra AK. Dynamics of structures: theory and applications to earthquake engineering. 3rd ed. New Jersey: Prentice Hall; 2007.
[70] Al Atik L, Sitar N. Seismic earth pressures on cantilever retaining structures. Journal of Geotechnical and Geoenvironmental Engineering 2010;136:1324–33.
[71] di Santolo AS, Evangelista A. Dynamic active earth pressure on cantilever retaining walls. Computers and Geotechnics 2011;38:1041–51.
[72] Prakash S. Soil dynamics. New York: McGraw Hill Book Company; 1981.
[73] Dewoolkar MM, Ko HY. Pak RYS. Seismic behavior of cantilever retaining walls with liquefiable backfills. Journal of Geotechnical and Geoenvironmental Engineering 2001;127(5):424–35.
[74] Kloukinas P, Penna A, di Santolo AS, Bhattacharya S, Dietz M, Dihoru L, Evangelista A, Simonelli AL, Taylor CA, Mylonakis G. Experimental investigation of dynamic behavior of cantilever retaining walls. Second international conference on performance-based design in earthquake geotechnical engineering, Taormina, Italy: May 28–30; 2012. Paper no. 13.08.
[75] PEER. 〈http://peer.berkeley.edu/svbin/GeneralSearch〉; 2012.
[76] Cosenza E, Manfredi G. Damage indices and damage measures. Progress in Structural Engineering and Materials 2000;2(1):50–9.
[77] Zhu TJ, Tso WK, Heidebrecht AC. Effect of peak ground a/v ratio on structural damage. Journal of Structural Engineering 1988;114(5):1019–37.
[78] Meskouris K, Kratzig WB, Hanskotter U. Seismic motion damage potential for R/C wall–stiffened buildings. In: Fajfar P, Krawinkler H, editors. Nonlinear seismic analysis and design of reinforced concrete buildings. Oxford: Elsevier Applied Science; 1992. p. 125–36.